

Charge-Exchanged Beam Measurement by Using a Grid-Biased Faraday Cup

Atsushi OKAMOTO, Takehiro ISONO, Tsuguhiro NISHIUCHI, Hiroyuki TAKAHASHI,
Sumio KITAJIMA and Mamiko SASAO

Tohoku University, Sendai 980-8579, Japan

(Received 8 December 2009 / Accepted 4 March 2010)

A method for neutral beam measurement by using a Faraday cup is proposed in this paper. The method enables us to detect neutral beams by controlling secondary electrons by using a biasing grid in front of the Faraday cup. A procedure is also proposed for *in situ* determination of the secondary electron emission coefficient of the Faraday cup. Experimental results show that appropriate emission coefficients are determined for helium beams with energies of 2-10 keV. The neutral flux charge-exchanged from a helium ion beam passing through a helium gas is also measured. Saturation of the neutral flux is observed above the pressure expected from the solution of a rate equation. The method is promising for neutral beam measurement, especially for small current-neutral beams.

© 2010 The Japan Society of Plasma Science and Nuclear Fusion Research

Keywords: neutral beam, charge exchange, secondary electron emission, grid-biased Faraday cup, rate equation

DOI: 10.1585/pfr.5.S2088

1. Introduction

Charge exchange is a significant process for transport phenomena of energetic particles in divertor plasmas. Studying those phenomena by using a small device with an energy-controlled beam [1] has experimental advantages such as flexibility and accessibility. Thus, methods for measurement of a small current-neutral beam ($I_{\text{beam}} \sim 1 \text{ nA} - 1 \mu\text{A}$) are required. While thermal methods are applied to high-current heating beams, it is difficult to apply them to a small current-neutral beam because of the small signal-to-noise ratio. A Faraday cup is a widely applicable tool but only for charged beams. A pyroelectric detector [2] is a candidate for measuring small current-neutral beams. However, it requires a pair of deflectors and free flight space to separate the neutral beam and ion beam components. Moreover, a slow time constant ($\Delta t \sim 1 \text{ s}$) sometimes limits its application.

In the present paper, a measurement method for separate measurement of a neutral beam current under ion beam mixing is proposed. The method uses a biasing grid in front of a Faraday cup, which controls the secondary electrons emitted from the Faraday cup. Thus, the detector is simple and compact. However, the method requires accurate coefficients for secondary electron emission. Thus, a procedure for obtaining these coefficients is also proposed, which allows *in situ* determination of the emission coefficient of the Faraday cup. In section 2, the principle of the measurement method and the determination of the emission coefficients are described. An experimental setup with a prototype of the neutral beam detector is presented in

section 3. The results and discussion are given in section 4; the determination of the emission coefficients is shown first, and then, the measured neutral and ion beam fluxes are presented. The paper is summarized in section 5.

2. Principle of Neutral and Ion Flux Measurement

A schematic of the Faraday cup with retarding grids is shown in Fig. 1. The closest grid, grid 1, controls the secondary electrons, while the others repel the electrons and ions of a bulk plasma. Usually the beam energy is sufficiently higher than the energy of the bulk electrons and ions in the plasma. Only the beam component can reach the collector as far as the grid 2 and 3 are suitably biased in positive and negative, respectively.

When grid 1 is biased with a sufficiently negative voltage, secondary electrons are completely suppressed. The collector current is derived by

$$I_c^- = eS\Gamma_i, \quad (1)$$

where S and Γ_i are the collecting area and beam-ion flux, respectively. On the other hand, when grid 1 is positively biased, the secondary electrons are completely emitted from the collector. The collector current is derived by

$$I_c^+ = eS(\Gamma_i + \eta\Gamma_i + \eta\Gamma_0), \quad (2)$$

where η and Γ_0 are the secondary electron emission coefficient and neutral flux, respectively. The coefficient η for neutral flux and that for ion flux are assumed to be the same for low energy ($\leq 10 \text{ keV}$) beams. Thus, the ion and

author's e-mail: atsushi.okamoto@qse.tohoku.ac.jp

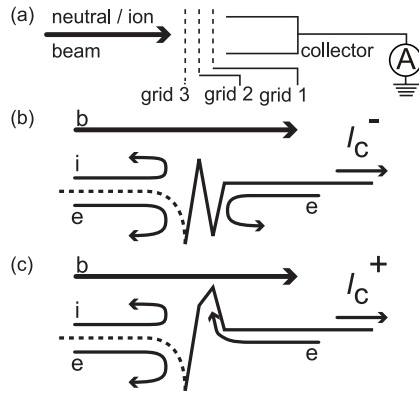


Fig. 1 (a) Schematic of the Faraday cup with retarding grids. (b) Potential profile for secondary electron suppression, where e stands for electrons, i for bulk ions, and b for beam components. (c) Potential profile for active emission of secondary electrons from the Faraday cup collector.

neutral flux are obtained using Eqs. (1) and (2).

$$eS\Gamma_i = I_c^-, \quad (3)$$

$$eS\Gamma_0 = [I_c^+ - (1 + \eta)I_c^-]/\eta. \quad (4)$$

Equations (3) and (4) show that the neutral beam flux can be measured using the Faraday cup.

On the other hand, the neutral beam flux in Eq. (4) is accurately measured when an appropriate emission coefficient η is given. In general, the emission coefficient sensitively depends on the surface conditions. Thus, *in situ* calibration is advantageous for determining the emission coefficient. Under the neutral flux-free condition, $\Gamma_0 = 0$, Eqs. (1) and (2) directly yield the emission coefficient,

$$\eta = I_c^+/I_c^- - 1. \quad (5)$$

The neutral flux-free condition is usually realized by injecting an ion beam that does not pass through target gases or target plasmas. Using the emission coefficient experimentally determined by Eq. (5), the neutral beam flux passing through the target is obtained in the same device.

3. Experimental Setup

Experiments have been performed using the DT-ALPHA device [3]. A Faraday cup equipped with three biasing grids is installed in the center of an end plate, as shown in Fig. 2. The collector of the Faraday cup is made of stainless steel and has an inner diameter of 8 mm and a depth of 18 mm. Three grids are installed with separate biasing voltage supplies. The three grids are made of molybdenum mesh; the mesh size is 0.03 mm in diameter and 150 meshes per inch. Each grid is separated from the others by a distance of about 3 mm.

A multicusp ion source [4, 5] is installed 2 m away from the Faraday cup at the other end of the device. The ion source has an inside volume 80 mm in diameter and 90-mm long. Permanent magnets attached to the wall form a

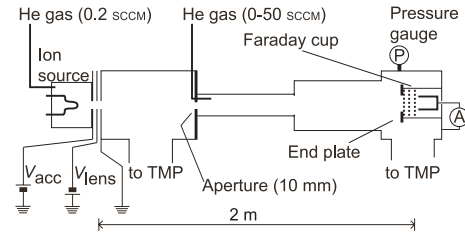


Fig. 2 Schematic of the experimental set up.

line cusp magnetic field for plasma confinement. Helium gas at 0.2 standard cubic centimeters per minute (SCCM) is injected into the ion source chamber. A hot tungsten filament serves as the cathode of an arc discharge. About 0.1 kW of arc power is injected into the ion source.

The ion source chamber is connected to the acceleration electrode, which is biased at a positive potential up to $V_{acc} = 10$ kV. The lens electrode between the acceleration electrode and the ground electrode, which is negatively biased at $-V_{lens}$ with respect to the ground electrode, is adjusted to the optimum beam current. Steady-state helium ion beams extracted from an extraction hole 6 mm in diameter are injected into the DT-ALPHA device.

A stainless steel aperture with an inner diameter of 10 mm is located at the entrance of the main chamber. Helium gas controlled through a mass flow controller is fed with a flow rate of up to 50 SCCM. Turbo molecular pumps are located at the upstream and down stream manifolds. The pressure is measured at the down stream manifold. Because of gas conductance, the working pressure in the main chamber is about three to ten times higher than that measured at the down stream manifold.

4. Results and Discussion

Helium ion beams with energies of 2-10 keV were injected into the DT-ALPHA device when it was filled with helium gas. Currents were measured using a Faraday cup with grids. The biasing potential of the grid in front of the Faraday cup (grid 1 in Fig. 1) was varied over a range of $V_{grid1} = \pm 50$ V to absorb and reflect secondary electrons. The pressure dependence of the Faraday cup current is shown in Fig. 3. Open circles indicate the current obtained for a negatively biased grid, and filled squares represent that for a positively biased grid. As the pressure increases, both currents attenuate but with different slopes. The difference in the slopes of the attenuation implies that the ratio of the neutral and ion beam components changes with the filling gas pressure. On the other hand, the currents gradually increase with the filling gas pressure up to $p < 0.005$ Pa. This is because the space charge of the ion beam is canceled by the weakly ionized ambient gas.

4.1 *In situ* calibration for secondary electron emission

To obtain the neutral beam flux, the coefficient of sec-

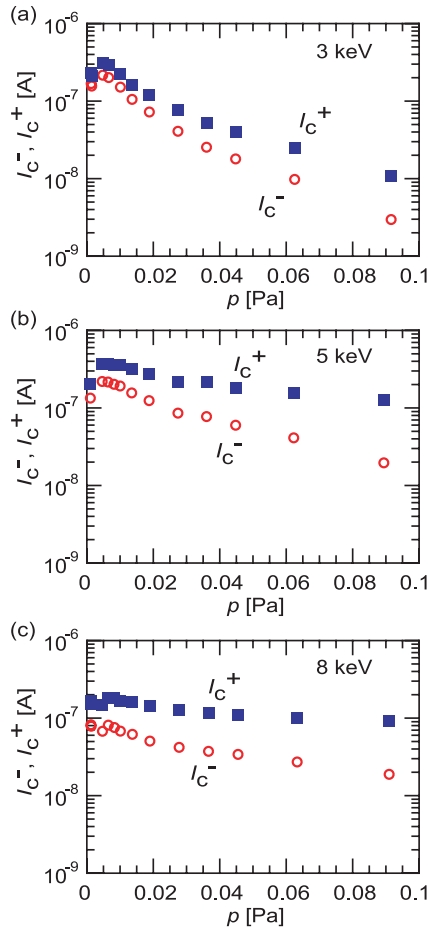


Fig. 3 Pressure dependence of collector current for beam energies of (a) 3 keV, (b) 5 keV, and (c) 8 keV. Open circles represent the current with secondary electron suppression [Fig. 1 (b)]. Filled squares represent the current with active emission of secondary electrons [Fig. 1 (c)].

secondary electron emission for the Faraday cup is experimentally determined. The coefficient is determined from the pure ion beam flux, which is realized at the limit of $p \rightarrow 0$. To avoid the space charge divergence effect, the pure ion beam flux is obtained by an extrapolation of the space charge compensated region (pressure range of $p = 0.005$ - 0.02 Pa). An exponential function is used for the extrapolation.

The secondary electron emission coefficient for each energy is obtained using Eq. (5), as shown in Fig. 4. The emission coefficient is on the order of unity and increases monotonically with the beam energy. The error is mainly caused by the extrapolation to $p \rightarrow 0$. The emission coefficients for other materials [6], which are also plotted in Fig. 4 as a reference, are on the order of unity and increase monotonically with the beam energy. The difference between the materials is considerably small. The emission coefficient of stainless steel in the present experiment is on the same order and agrees qualitatively with that for those materials. These results indicate that *in situ* determination of the emission coefficient is efficient.

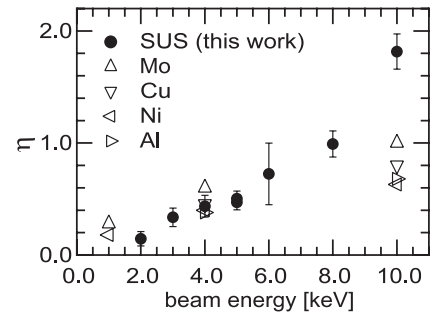


Fig. 4 Energy dependence of secondary electron emission coefficient.

On the other hand, the emission coefficient of stainless steel is slightly smaller than that of the other materials at low energy and is higher than the others at high energy. A possible cause is the surface conditions. While the emission coefficient of stainless steel is measured when it is a component of the Faraday cup, the other materials were carefully prepared to measure the emission coefficient of a clean surface. Since the emission coefficient of the Faraday cup is needed to obtain the neutral beam flux, applying the *in situ* determination of the emission coefficient of the Faraday cup is preferable.

4.2 Neutral and ion flux measurement

After determining the emission coefficient, the neutral and ion beam fluxes are obtained using Eqs. (3) and (4). The pressure dependence of the neutral and ion beam fluxes is shown in Fig. 5. The neutral beam flux increases with pressure because of the increase in the charge-exchange rate and then saturates or gradually decreases. The ion beam flux, which is the same as the Faraday cup current obtained for a negatively biased grid (open circles in Fig. 3), decreases by charge exchange with increasing pressure. The sum of the ion and neutral fluxes decreases gradually with increasing pressure. The steeper slope in the lower-energy beam is caused by divergence of the beam due to elastic scattering. The cross section of elastic scattering is large for a low-energy beam.

The ion beam flux has two slopes, a steep one at low pressure ($p \leq 0.02$ Pa) and a moderate one at high pressure ($p \geq 0.03$ Pa). The boundary of these two regions coincides with the change in the neutral flux behavior from the increasing phase to the saturated (or gradually decreasing) phase. The pressure dependence of the ion and neutral fluxes is regarded as having a spatial evolution, since the horizontal axis in Fig. 5 represents an equivalent distance at a constant pressure. Thus, the boundary implies a transition from a single collision to multiple collisions. While charge exchange with a target gas decreases the ion beam flux and increases the neutral beam flux, ionization of the neutral beam by collisions with the target gas decreases the neutral beam flux and increases the ion beam flux. In the present experiment, the initial beam is purely an ion beam.

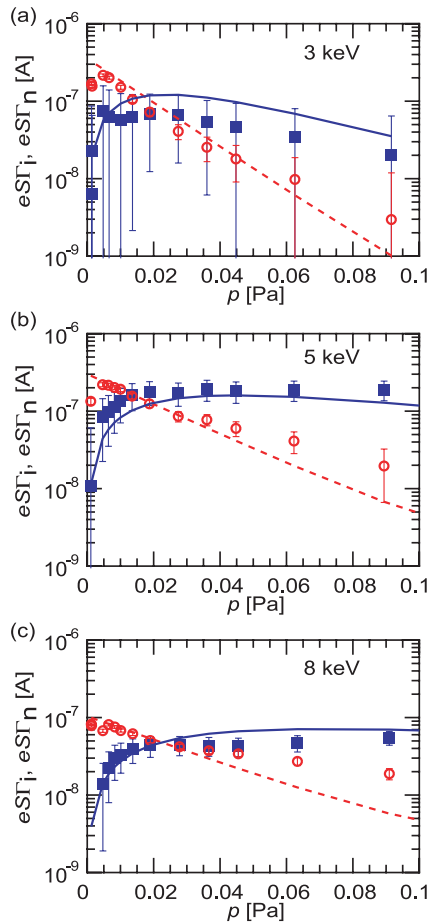


Fig. 5 Pressure dependence of neutral and ion fluxes for beam energies of (a) 3 keV, (b) 5 keV, and (c) 8 keV. Filled squares represent neutral flux; open circles represent ion flux. Solid and dashed curves represent the solution of a rate equation for the neutral and ion fluxes, respectively.

Thus, charge exchange from the ions to the neutrals occurs rapidly. After an adequate neutral beam is produced, ionization effectively transforms it to an ion beam. This is qualitatively true; since the cross section of the charge exchange is on the order of $\sigma \sim 10^{-15} \text{ cm}^2$, the mean free pressure is $p \sim k_B T / \sigma L \sim 0.04 \text{ Pa}$ in an $L \sim 1 \text{ m}$ device.

To confirm the discussion above, a set of rate equations is solved. Assuming a constant gas pressure, the spatial evolution of the ion and neutral fluxes is considered. Elastic scattering and charge exchange are the loss terms for the ion flux, and ionization is the production term. Elastic scattering and ionization are the loss terms for the neutral flux, and charge exchange is the production term. Under an initial condition of neutral flux-free injection, the rate equation is analytically solved. The results are shown in Fig. 5. While the ion beam monotonically decreases,

the neutral flux increases with pressure and then saturates or gradually decreases. Those curves effectively represent the experimental behavior. In addition to the qualitative explanation, the absolute values are almost within the experimental errors except for the ion flux at high pressure. The reason for the underestimation of the ion flux at high pressure is unclear, and examining it remains our future work, which will require the spatial distribution of the filled gas density along the beam pass. At least the result of the rate equation calculation indicates that the change in neutral flux behavior observed in the experiment is evidence of the change from a single collision to multiple collisions.

5. Summary

A method for neutral beam measurement using a Faraday cup is proposed. The method enables us to detect neutral beams by controlling secondary electrons by using a biasing grid in front of the Faraday cup. A procedure is proposed to obtain the secondary electron emission coefficient of the cup material as a component of the Faraday cup. Experimental results show that appropriate emission coefficients are determined for beam energies of up to 10 keV. A neutral flux produced by charge exchange with a helium ion beam passing through helium gas is also measured. Saturation of the neutral flux is observed above the pressure expected from the solution of a rate equation. The method is suitable for neutral beam measurement, especially small current-neutral beams.

Acknowledgment

This study was partly supported by a Ministry of Education, Culture, Sports, Science and Technology of Japan (MEXT) Grant-in-Aid for the “priority area of Advanced Burning Plasma Diagnostics” (16082201).

- [1] A. Okamoto, T. Isono, T. Kobuchi, S. Kitajima and M. Sasao, *J. Plasma Fusion Res. SERIES* **8**, 39 (2009).
- [2] A. Viehl, M. Kanyo, A. van der Hart and J. Schelten, *Rev. Sci. Instrum.* **64**, 732 (1993).
- [3] A. Okamoto, K. Iwazaki, T. Isono, T. Kobuchi, S. Kitajima and M. Sasao, *Plasma Fusion Res.* **3**, 059 (2008).
- [4] K. Shinto, H. Sugawara, M. Takenaga, S. Takeuchi, N. Tanaka, A. Okamoto, S. Kitajima, M. Sasao, M. Nishiura and M. Wada, *Rev. Sci. Instrum.* **77**, 03B512 (2006).
- [5] H. Sugawara, K. Shinto, N. Tanaka, S. Takeuchi, M. Kikuchi, A. Okamoto, S. Kitajima, M. Sasao and M. Wada, *Rev. Sci. Instrum.* **79**, 02B708 (2008).
- [6] *Atomic Data for Controlled Fusion Research III* (ORNL-6088), Ed. by E. W. Thomas, (Oak Ridge National Laboratory, USA, 1985) Chapter C.